Proceedings of the ASME 2023 43rd International Conference on Ocean, Offshore and Arctic Engineering
OMAE2024
June 9-14, 2024, Singapore EXPO, Singapore

OMAE2024-128231

DATA DRIVEN IDENTIFICATION AND MODEL PREDICTIVE CONTROL FOR A CATAMARAN SURFACE VESSEL

Vallabh Deogaonkar[1,*], Mohammed Ibrahim M[1], Akash Vijayakumar[1], Abhilash Somayajula[1,*]

[1]Marine Autonomous Vessels Laboratory,Indian Institute of Technology (IIT) Madras,Chennai,India

ABSTRACT

Autonomous Surface Vehicles (ASVs) have received increasing attention in various maritime applications over the years. Their ability to operate autonomously in complex and confined environments, such as narrow inland waterways, presents a unique set of opportunities and challenges. This paper presents a comprehensive study on the dynamics identification and subsequent development of a Model Predictive Controller (MPC) for a catamaran surface vessel. The catamaran surface vessel under investigation was fabricated in-house with a holonomic thruster configuration and a comprehensive sensor suite. This study focuses on experimental identification of a 3 degree of freedom maneuvering model of the fully actuated surface vessel. With a well-defined dynamic model in place MPC is designed for efficiently tracking a path while maintaing surge velocity. The MPC framework is chosen due to its ability to optimize control inputs over a finite prediction horizon, ensuring the catamaran follows desired trajectories while adhering to operational constraints and actuator constraints. This paper outlines a holistic study on the dynamics identification and MPC development of an ASV to impact a wide range of applications, from oceanographic research to coastal security, by providing a robust control framework that can navigate the challenges of dynamic marine environments.

Keywords: System Identification, Abkowitz model, Model Predictive Control

1. INTRODUCTION

Autonomous Surface Vehicles (ASVs) have emerged as highly versatile platforms, finding applications in critical domains such as flood relief operations[1]. Additionally, ASVs also hold potential to contribute significantly to bathymetric surveys in ports and oceanography, playing a pivotal role in environmental and maritime research [2]. Other innovative applications include surveillance[3] and Autonomous Underwater Vehicle (AUV) navigation assistance[4]. In all such applications, the vessel needs to navigate autonomously in confined maritime environments with enhanced maneuverability. Unlike traditional cargo ships which are predominantly underactuated, fully actuated surface vessels can achieve superior maneuverability due to presence of multiple control inputs and hence are more suited for such applications.

To successfully achieve the above objectives using ASVs, requires accurate understanding of their dynamic models so that it can be used to develop efficient controllers. Numerous studies have delved into model identification for surface vessels, aiming to enhance our understanding of these dynamic systems. Noteworthy mentions include investigations into fully actuated vessels, such as the Wave Adaptive Modular Vessel (WAMV)[5] as well as under-actuated surface vessels [6]. But traditional approaches often involve laborious and resource-intensive experimental processes. Obtaining a mathematical model such as MMG [7] also requires extensive experiments in specialised facilities, which are not universally accessible. Alternatively approaches using computational tools such as CFD [8] are time consuming and require precise modelling of the geometry of the vessel. Yet, these studies contribute valuable insights into the development of dynamic models for ASVs. In this study, the challenge of model identification of ASV is explored using data driven methodology. Free running maneuvers are utilised, to circumvent the challenges associated with the requirement of specialised facilities. One of the key advantages of using such data driven methods is that these experiments represent the dynamics of the vessel in its purest form without needing to conduct separate experiments to capture interactions of hull and control surfaces. Furthermore, no prior information of the parameters of the ASV such as its mass or geometric parameters are assumed. Once the dynamic model is identified, it becomes a pivotal tool for subsequent phases of control system development.

Applications such as flood relief and bathymetry require precise maneuvering control while also reducing the controller effort. One of the prominent methodologies that can be used to achieve this is the MPC[9] and it has received considerable attention over the years. MPC optimizes control inputs over a finite prediction horizon such that the operational requirements are met, while also adhering to the controller and physical constraints. The predictive

*Corresponding author: oe23d002@smail.iitm.ac.in, abhilash@iitm.ac.in

nature of MPC, distinguishes it from traditional control methods and contributes to its efficacy. An accurate modelling of system dynamics aids in better predictive capability and hence better controller performance. Another advantage of MPC over other control algorithms [10] becomes evident in its adept handling of constraints. MPC excels at ensuring control within predefined limits which can be either physical limitations of the system or operational constraints. This quality is particularly valuable in applications where precise control is paramount, such as the navigation of ASVs through intricate waterways [11].

This paper underscores MPC as one of the best applications of the obtained ASV hydrodynamic model. By combining the accessibility of free running model tests for system identification with the optimization capability of MPC, this paper demonstrates a comprehensive framework for enhancing ASV maneuverability and performance. This integrated approach holds promise for advancing the field, with applications extending from oceanographic research to coastal security.

The rest of the paper is organised as follows : section 2 provides the details of fully actuated catamaran surface vessel used in this study, section 3 covers the details of vessel dynamics modelling along with the kinematics and kinetics, section 4 covers the methodology used for identifying the dynamics of the vessel using free running maneuvering data, section 5 provides the details about formulation of MPC and simulation results, section 6 concludes the paper by summarizing the key results and plans for future works.

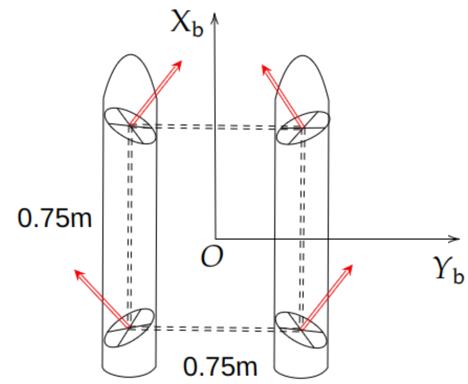

FIGURE 2: X-Thruster configuration

2. ARITRA : AUTONOMOUS SURFACE VESSEL

FIGURE 1: Aritra : Autonomous surface vessel

The vessel used in this study to demonstrate the methodology of system identification and the subsequent application of Model predictive control is shown in Figure 1. This vessel named Aritra is of catamaran type and it is fully actuated in all three modes of surge, sway and yaw. The individual hull dimensions are 1.47m x 0.25m x 0.16m with a separation of 0.25m between the two hulls. The vessel is controlled using four T200 thrusters, 2 on each hull placed at 45 degrees in a holonomic X configuration [12] as shown in Figure 2.

The vessel is also equipped with a comprehensive sensor suite consisting of an IMU sensor, a GPS sensor, a 2D Lidar, and a stereo camera. For testing the vessel in wave-basin facility at IIT Madras, where the GPS positioning is not accurate, the vessel is also equipped with a UWB based indoor localisation module developed inhouse. This module consists of four stationary anchors and a movable tag which can be used for indoor positioning. The primary processor onboard is a Jetson Nano with Ubuntu 20 operating system and ROS Noetic as the middleware for sensor integration.

3. VESSEL DYNAMICS

The dynamics of a surface vessel is influenced by its interaction with the surrounding water. These hydrodynamic interactions are complex and nonlinear in nature and they are influenced by various factors such as the vessel's hull form geometry, propulsion mechanism and the presence of various control surfaces. The study of ship maneuvering aims to model these interactions in a simplified manner using the Newton's laws of motion and expressing them with a set of simple differential equations. This simplification is essential for quickly simulating vessel dynamics and for designing and testing different controllers [13]. These differential equations include the vessel position and velocity as variables and comprise of various linear and nonlinear terms. Collectively, these equations are termed as the maneuvering equations of motion and they encompass both kinematics and dynamics of the surface vessel. In this study, the 3 DOF maneuvering model of the surface vessel in surge, sway and yaw is considered. For a catamaran surface vessel, the stability in seakeeping modes of roll, pitch and heave motions is greater as a result of increased waterplane area compared to monohull. Moreover these seakeeping modes are not controllable using the actuators onboard the vessel. So, focus has been given to identification of dynamics in maneuvering modes of surge, sway and yaw.

3.1 Kinematics

Two frames of reference are considered in maneuvering equations for the surface vessel in this study. A global coordinate system (GCS) frame $O_0 - X, Y, Z$ and a body-fixed coordinate system (BCS) frame $O - x_b, y_b, z_b$ as seen in Figure 3. The kinematics of ship motion which relates the variables from these two coordinate frames are given by (1).

$$
\begin{aligned}
\dot{\boldsymbol{\eta}} &= [R(\psi)]\boldsymbol{\nu} \\
\boldsymbol{\nu} &= \begin{bmatrix} u \ v \ r \end{bmatrix}^T \\
\boldsymbol{\eta} &= \begin{bmatrix} x_G \ y_G \ \psi \end{bmatrix}^T \\
R(\psi) &= \begin{bmatrix} \cos(\psi) & -\sin(\psi) & 0 \\ \sin(\psi) & \cos(\psi) & 0 \\ 0 & 0 & 1 \end{bmatrix}
\end{aligned} \tag{1}
$$

where, $\boldsymbol{\nu}$ denotes the vector of state derivatives expressed in BCS and $\boldsymbol{\eta}$ denotes the vector of states expressed in GCS. $R(\psi)$ represents the rotation matrix such that any vector in BCS when pre-multiplied by this rotation matrix results in the same vector expressed in GCS. The surge (u), sway (v), and yaw (r) velocities are the state variables in the maneuvering equations of motion and they are measured in the body-fixed frame while the heading of the vessel (ψ) is given by the angle between the X-axes of the BCS and GCS. The position of the vessel in GCS at any time is given by its coordinates (x_G, y_G). Both the BCS and GCS frames have their z axis pointing downwards and it follows the popular North-East-Down (NED) convention.

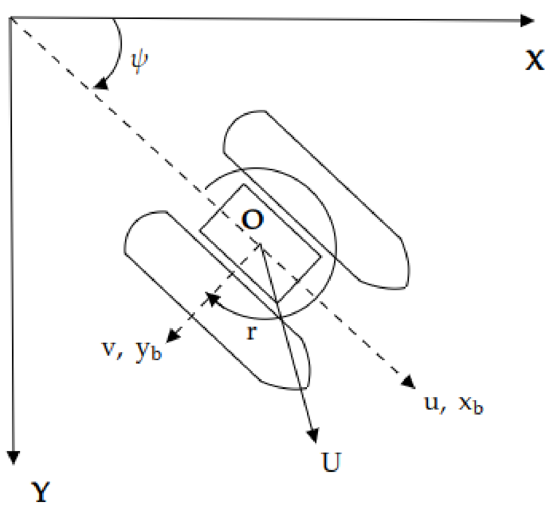

FIGURE 3: Ship coordinate frames and kinematic variables

3.2 Dynamics

As described in [14], the nonlinear dynamics of a surface vessel in the 3 DOF of surge, sway and yaw can be expressed using (2)

$$M\dot{\mathbf{v}} + C(\mathbf{v})\mathbf{v} + D(\mathbf{v})\mathbf{v} = \tau + \tau_d \tag{2}$$

The above expression is essentially Newton's second law expressed in the BCS frame. Here M is the rigid body and added mass matrix, C is the Coriolis-centripetal matrix, D is the damping matrix, τ is the vector of force and moments due to control inputs and τ_d is the vector of forces and moments due to external disturbances such as wind and waves. Since these equations of motion are expressed in BCS which is a non-inertial frame, Coriolis forces are included. It should be noted that both the Coriolis-centripetal and the damping matrix are functions of the velocity vector ($\mathbf{v}$) of the vessel whose components are u, v and r as expressed in (1). These two functions contribute to the non linearity in the dynamics. When expressing maneuvering equation of motion in calm water, τ_d can be neglected and (2) can be rewritten in terms of the components of $\mathbf{v}$ in the following form

$$
\begin{aligned}
\dot{u} &= f_X(u, v, r, t_x, t_y, t_n) \\
\dot{v} &= f_Y(u, v, r, t_x, t_y, t_n) \\
\dot{r} &= f_N(u, v, r, t_x, t_y, t_n)
\end{aligned} \tag{3}
$$

where f_X, f_Y and f_N are nonlinear functions which need to be identified using the system identification methodology. t_x, t_y and t_n are resultant local forces and moments in surge, sway and yaw due to the control inputs. For the vessel considered in this study these local forces arise due to the thruster commands given by the controller. Similar to Abkowitz model [15] the nonlinear functions f_X, f_Y and f_N can be expressed using their Taylor series approximations as shown in (4) around a nominal state of $u = 0.5, v = 0, r = 0$ and $\Delta u = u - 0.5$

$$
\begin{aligned}
\dot{u} = {} & X_0 + X_u\Delta u + X_v v + X_r r + X_{uu}\Delta u^2 + X_{vv}v^2 + X_{rr}r^2 \\
& + X_{uv}\Delta u v + X_{ur}\Delta u r + X_{vr}vr + X_{uuu}\Delta u^3 + X_{vvv}v^3 \\
& + X_{rrr}r^3 + X_{uuv}\Delta u^2 v + X_{uur}\Delta u^2 r + X_{vvu}v^2\Delta u \\
& + X_{vvr}v^2 r + X_{rru}r^2\Delta u + X_{rrv}r^2 v + X_{uvr}\Delta u v r \\
& + X_x t_x + X_y t_y + X_n t_n
\end{aligned} \tag{4a}
$$

$$
\begin{aligned}
\dot{v} = {} & Y_0 + Y_u\Delta u + Y_v v + Y_r r + Y_{uu}\Delta u^2 + Y_{vv}v^2 + Y_{rr}r^2 \\
& + Y_{uv}\Delta u v + Y_{ur}\Delta u r + Y_{vr}vr + Y_{uuu}\Delta u^3 + Y_{vvv}v^3 \\
& + Y_{rrr}r^3 + Y_{uuv}\Delta u^2 v + Y_{uur}\Delta u^2 r + Y_{vvu}v^2\Delta u \\
& + Y_{vvr}v^2 r + Y_{rru}r^2\Delta u + Y_{rrv}r^2 v + Y_{uvr}\Delta u v r \\
& + Y_x t_x + Y_y t_y + Y_n t_n
\end{aligned} \tag{4b}
$$

$$
\begin{aligned}
\dot{r} = {} & N_0 + N_u\Delta u + N_v v + N_r r + N_{uu}\Delta u^2 + N_{vv}v^2 + N_{rr}r^2 \\
& + N_{uv}\Delta u v + N_{ur}\Delta u r + N_{vr}vr + N_{uuu}\Delta u^3 + N_{vvv}v^3 \\
& + N_{rrr}r^3 + N_{uuv}\Delta u^2 v + N_{uur}\Delta u^2 r + N_{vvu}v^2\Delta u \\
& + N_{vvr}v^2 r + N_{rru}r^2\Delta u + N_{rrv}r^2 v + N_{uvr}\Delta u v r \\
& + N_x t_x + N_y t_y + N_n t_n
\end{aligned} \tag{4c}
$$

4. SYSTEM IDENTIFICATION

The goal of system identification is to identify all the coefficients in (4) of the form $X_{(.)}, Y_{(.)}$ and $N_{(.)}$ using the trajectory data collected from free running experiments as shown in [16]. The trajectory data consists of time series of velocity in surge (u), sway (v) and yaw rate (r) along with t_x, t_y and t_n, which are the resultant local forces and moments in surge, sway and yaw due to the control inputs.

4.1 Data collection methodology

The focus of this study was to first identify the calm water hydrodynamics of the surface vessel. Hence all the free running experiments were performed in the IIT Madras wave-basin facility in absence of wind and wave disturbances as shown in Figure 4. To identify the maneuvering performance of the vessel in presence of waves requires determination of wave-drift forces [17] and will be explored in future works. The dimensions of the wave basin are 30m x 30m x 3m. The primary sensors used for data collection were the UWB localisation module and IMU whose specifics are mentioned in Table 1.

TABLE 1: Sensors

Sensor	Measure	Frequency
Cube Orange Autopilot-IMU	r , ψ , a_x, a_y	30 Hz
UWB Pro-Indoor Localization	(X, Y) coordinates	1 Hz

It can be noted that none of the sensors onboard the vessel directly measured its surge, sway velocity. Moreover, the frequency of position data from UWB module was quite low as compared to yaw rate, hence a simple kinematics based Kalman filter [18] was used to estimate the surge and sway velocities at 10 Hz.

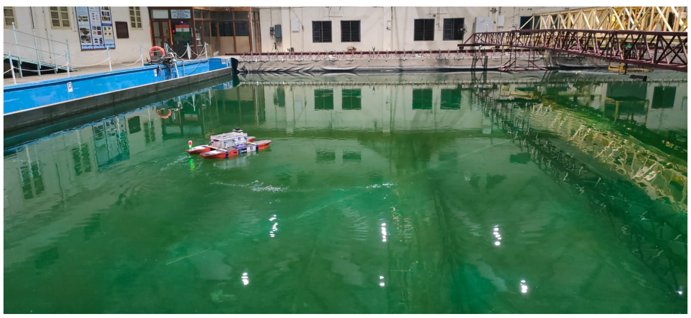

FIGURE 4: Free running test in wave basin

As discussed in section 3 the hydrodynamic force functions are being approximated using the Taylor series expansion. This approximation is representative of only those hydrodynamic interactions that are similar to the ones present in the training trajectory dataset. So the trajectory data should have all such interactions which are of interest to us. In order to collect a diverse set of the trajectory data, a teleoperation node was setup through ROS to maneuver the vessel. This teleoperation node used keyboard inputs corresponding to local forces and passed the required PWM commands to the thrusters. The mapping between the PWM commands and thrust force from the T200 thrusters was obtained from BlueRobotics website. [19]

One of the sample trajectories from the data used for identification is shown in Figure 5. The X-Y trajectory shown is generated using UWB localisation module and the velocity time series data predicted using the Kalman filter is shown in Figure 6. Since the Kalman filter was based on kinematics model alone, the estimated surge and sway velocities had considerable noise and a 1D Lanczos filter [20] was used to filter the data. Using this filtered time-series data, the acceleration terms of $\dot{u}$, $\dot{v}$ and $\dot{r}$ from (4) were computed at each sample times using 7 point forward, central and backward differences. Several such free running experiments were performed and a total of 13,840 data points were collected from these to identify the maneuvering model coefficients.To simplify the process of model identification, the data corresponding to local sway force commands was not included. Such data needs to be incorporated with a better methodology and is considered as the scope for future work on this vessel.

FIGURE 5: Sample free running trajectory

4.2 Formulation as linear regression problem

The nonlinear expressions from (4) can be expressed as a set of linear regression problems. These expressions can be written in the form shown in (5)

$$b = \mathbf{A}x \tag{5}$$

where b is a column vector of values of $\dot{u}, \dot{v}$ or $\dot{r}$ for all the data points, $\mathbf{A}$ is a matrix whose columns are the parameters in terms of u, v, r, t_x, t_y, t_n corresponding to each coefficient to be identified as shown in (6a) and x is a vector of coefficients to be estimated as shown in (6b) for the surge equation of motion. The coefficient vectors for sway and yaw are similar.

$$\begin{aligned}\mathbf{A}(k) = [&1, \Delta u(k), v(k), r(k), \Delta u^2(k), v^2(k), r^2(k),\\ &\Delta u(k)v(k), \Delta u(k)r(k), v(k)r(k), \Delta u^3(k), v^3(k),\\ &r^3(k), \Delta u^2(k)v(k), \Delta u^2(k)r(k), v^2(k)(k),\\ &v^2(k)r(k), r^2(k)\Delta u(k), r^2(k)v(k),\\ &u(k)v(k)r(k), t_x(k), t_y(k), t_n(k)]_{1\times 23}\end{aligned} \tag{6a}$$

$$\begin{aligned}X_c = [&X_0, X_u, X_v, X_r, X_{uu}, X_{vv}, X_{rr},\\ &X_{uv}, X_{ur}, X_{vr}, X_{uuu}, X_{vvv}, X_{rrr},\\ &X_{uuv}, X_{uur}, X_{vvu}, X_{vvr}, X_{rru}, X_{rrv},\\ &X_x, X_y, X_n]^T_{23\times 1}\end{aligned} \tag{6b}$$

where $A(k)$ represents one row of the matrix and k corresponds to the index of the data point. It should be noted that this system of equations has many more equations than unknowns (coefficients). Such a system is known as an overdetermined system. The solution obtained from linear regression in such a case is the one that minimizes the mean squared error between the true values and the predicted values. The least squares solution for an overdetermined system can be found analytically using (7)

$$x = (\mathbf{A}^T\mathbf{A})^{-1}\mathbf{A}^T\mathbf{b} \tag{7}$$

The identified coefficients for surge, sway and yaw are reported in Table 2. Using the identified coefficients the vessel motion was simulated and the resulting trajectory was compared against test experimental trajectory which was not included in the training with the same open loop control commands for both.

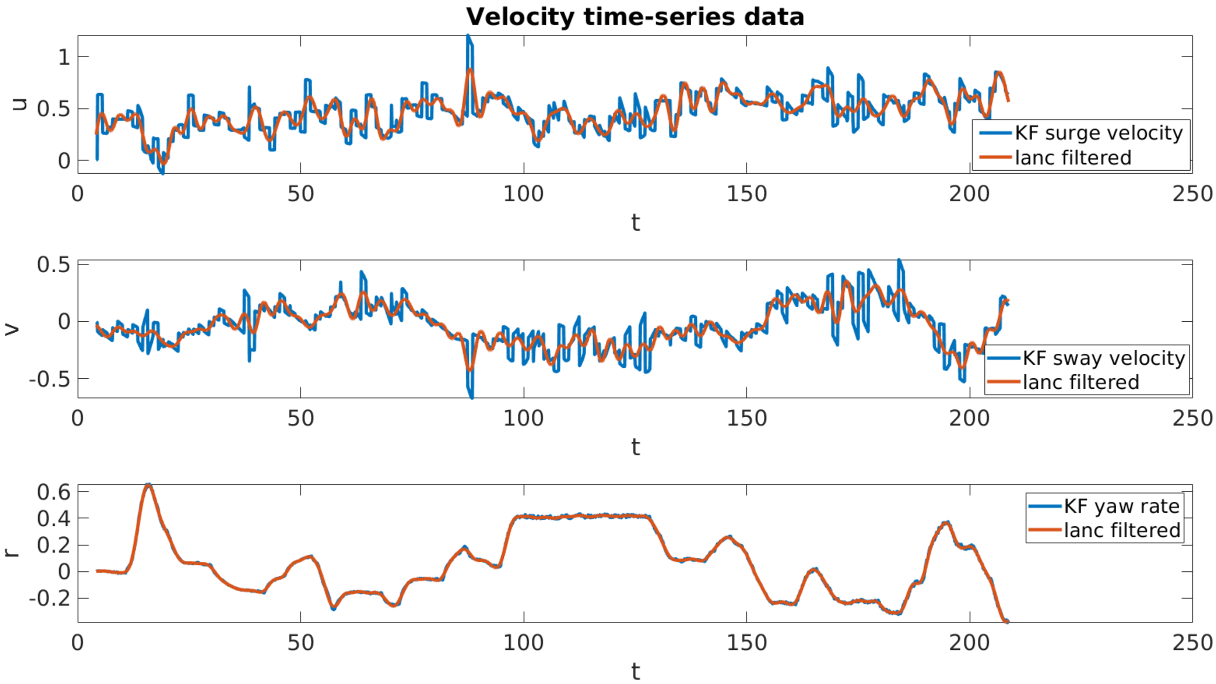

FIGURE 6: Velocity time series with Lanczos filtering

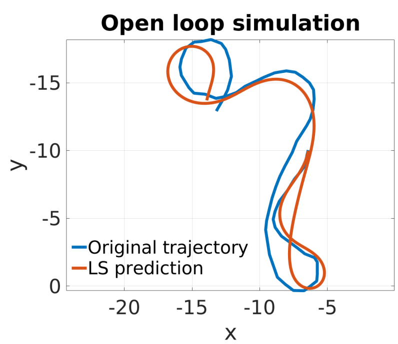

FIGURE 7: Comparison of X-Y trajectory

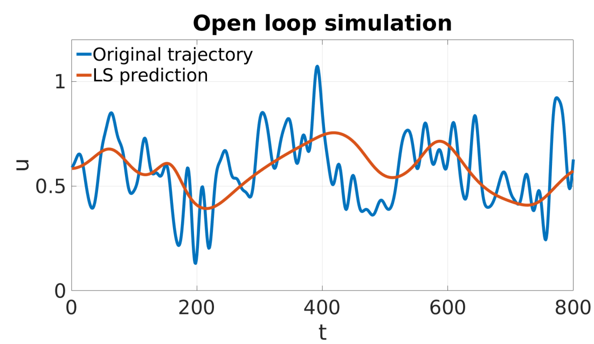

FIGURE 8: Surge velocity comparison

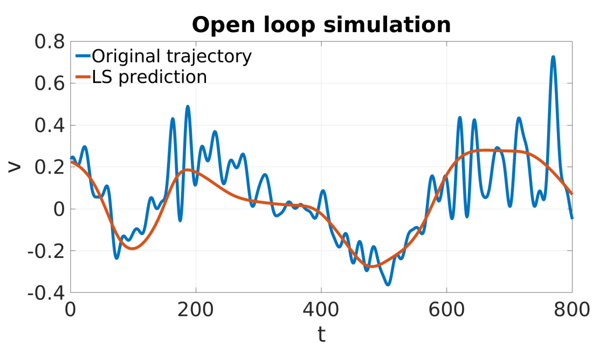

FIGURE 9: Sway velocity comparison

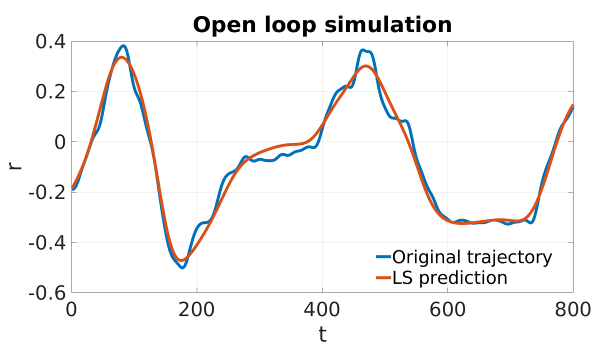

FIGURE 10: Yaw rate comparison

TABLE 2: Identified Hydrodynamic coefficients

Coefficient	Surge	Sway	Yaw
C_0	0	0	0
C_u	-0.0472	0.0016	0.0179
C_v	-0.0022	-0.0542	0.0174
C_r	-0.0693	0.0312	-0.2562
C_{uu}	0.1222	0.1106	0.0426
C_{vv}	0.1493	-0.0198	0.0310
C_{rr}	-0.1172	-0.0639	-0.0251
C_{uv}	-0.3011	-0.5449	-0.0913
C_{ur}	-0.0867	-0.7225	0.0263
C_{vr}	0.5930	-0.1211	0.0644
C_{uuu}	-0.1993	-0.4348	-0.0256
C_{vvv}	0.0745	0.2863	-0.0777
C_{rrr}	0.1971	0.0361	-0.7737
C_{uuv}	0.3562	0.4971	0.0576
C_{uur}	-0.2348	-0.6637	0.0292
C_{vvu}	0.5726	-0.0834	-0.0184
C_{vvr}	-0.1181	0.5999	-0.5678
C_{rru}	0.4229	0.1556	0.0404
C_{rrv}	-0.2630	0.0864	0.1086
C_{uvr}	1.8988	-0.1744	0.3863
C_x	0.0089	-0.0011	-0.00064
C_y	0	0	0
C_n	0.0279	-0.1132	0.3873

The result of comparison between the trajectories is shown in Figure 7. The comparison plots of time series of surge, sway velocities and yaw rate for the open loop trajectory are shown in Figure 8, Figure 9 and Figure 10. It can be noted that the identified model does not represent the noise present in the experimental predictions of surge and sway velocities but captures the overall trend of the variation decently well. The noise seen in experimental data is attributed to UWB sensor noise and not wave frequency motion because the tests were conducted in the wave basin facility in absence of all wave and wind disturbances. It can also be noted that the noise is present only in the surge and sway velocity estimates which are estimated using UWB sensor and not in the yaw rate.

5. MODEL PREDICTIVE CONTROL

Model Predictive Control (MPC) is a sophisticated control strategy designed to handle complex systems with predictive capabilities. The core concept revolves around iteratively solving an optimization problem at each time step to determine the optimal control inputs for the system over a finite prediction horizon. This predictive horizon allows MPC to foresee future states, enabling precise and adaptable control in real-time.

The optimization problem in MPC typically involves minimizing a cost function, which combines terms representing the desired state trajectory, control effort, and deviations from system constraints. The cost function serves as a measure of system performance, and its minimization guides the selection of optimal control inputs. The optimization is subject to system dynamics, state-space constraints, and input constraints, ensuring that the control inputs adhere to the system's limitations.

Mathematically, the MPC algorithm can be represented as follows:

$$\min_{C} J = \sum_{k=0}^{N-1} L(x_k, c_k) \tag{8a}$$

$$\begin{aligned} \text{subjected to:} \quad x_{k+1} &= f(x_k, c_k) \\ x_{\min} &\le x_k \le x_{\max} \\ c_{\min} &\le c_k \le c_{\max} \end{aligned} \tag{8b}$$

Where,

- J is the cost function,
- L represents the stage cost at each time step,
- x_k is the system state at time k,
- c_k is the control input at time k,
- f denotes the system dynamics,
- N is the prediction horizon,
- $x_{\min}, x_{\max}, c_{\min}$, and $c_{\max}$ are state and control input constraints.

The predictive nature of MPC ensures that it can accommodate systems with non-linear dynamics and handle constraints effectively. In the context of ASVs, this capability becomes crucial for precise trajectory tracking, especially in dynamic marine environments. The iterative nature of MPC allows it to continuously refine the control strategy based on real-time feedback, making it a powerful and adaptable control framework.

5.1 Formulation of the optimisation problem

Using the identified dynamics model in section 4, MPC was implemented for tracking a series of waypoints while maintaining a constant surge velocity. This subsection details the formulation of the optimisation problem to achieve this task.

To track the series of waypoints while maintianing a constant surge velocity, the cost function J and controller constraint were defined as follows,

$$\begin{aligned} J = \sum_{k=0}^{N-1} & s_u(u(k) - u_{des})^2 + s_\psi(\psi(k) - \psi_{des})^2 \\ & + s_v(v(k) - v_{des})^2 + s_c \sum_{i=1}^{4} (c_i(k))^2 \end{aligned} \tag{9a}$$

$$c_{\min} \le c_k \le c_{\max} \tag{9b}$$

where,

- $u(k)$, $v(k)$ and $\psi(k)$ denote the surge velocity, sway velocity and heading angle of the vessel respectively in the k^{th} step of the prediction horizon.
- $c_i(k)$ denotes the controller effort of the i^{th} thruster at k^{th} step of the prediction horizon.

- Desired surge velocity u_{des} for tracking was set to 0.5 m/s.
- Desired sway velocity v_{des} for tracking was set to 0 m/s.
- Desired heading angle ψ_{des} at each evaluation of MPC was assumed to be constant for the entire prediction horizon and was obtained using LOS guidance law.
- s_u, s_v , s_ψ and s_c denote the scaling factors for the corresponding costs and their values were chosen to be 2, 1, 1 and 0.001 respectively.
- Prediction horizon N was set to 10.
- The identified model of the vessel was used in MPC throughout the prediction horizon and no further constraints were imposed on the other states.
- Constraint on upper and lower bound of thrust force for each thruster was imposed with c_{min} = -4.0793 and c_{max} = 5.1536. These limits were imposed based on the data of PWM vs thrust force available for the T200 thrusters.

To address the constrained nonlinear optimization problem as formulated above, the nlpsol function from CasADi 3.6.4 [21] was employed, utilizing the ipopt solver. After running the optimisation and finding optimal control actions for 10 steps of the prediction horizon, only the first was used before restarting the evaluation. As more data will be collected in future to improve the accuracy of the identified model, the number of optimal actions used can be increased. This will help in reducing the frequency of evaluations of the optimisation problem and make the implementation computationally less expensive.

5.2 Simulation results

The optimal control inputs obtained using model predictive control were used for tracking the sequence of waypoints as shown in Figure 11. The corresponding plots of surge velocity and the controller effort are shown in Figure 12 and Figure 13. Figure 14 shows a magnified view of the controller effort in each of the 4 thrusters during a turn. These simulation results act as a baseline for comparing against the experiments. Due to unavailability of experimental data at the time of writing this paper, the comparison is planned for future work.

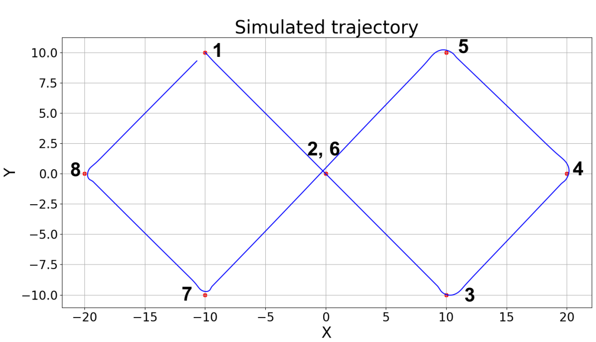

FIGURE 11: Simulated trajectory tracking using MPC

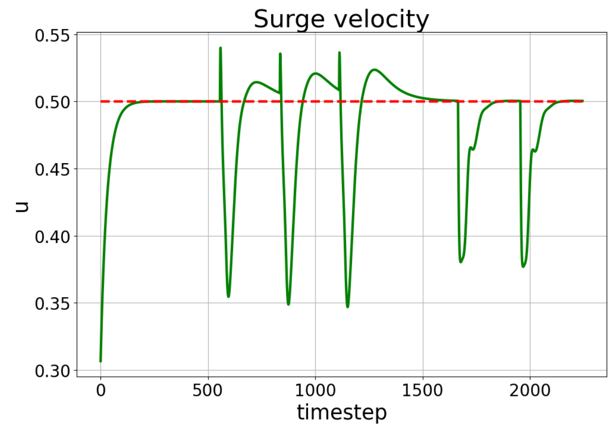

FIGURE 12: Surge velocity with reference value 0.5

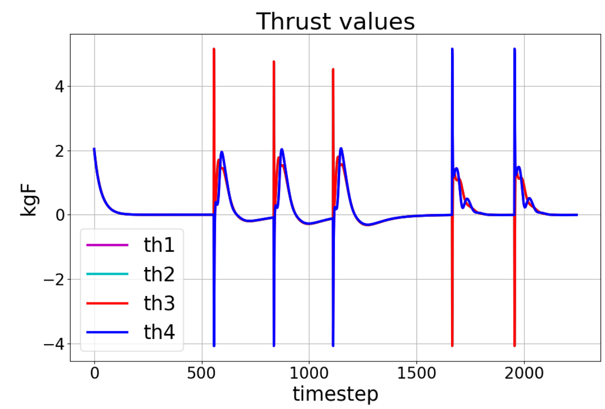

FIGURE 13: Controller effort when s_c = 0.001

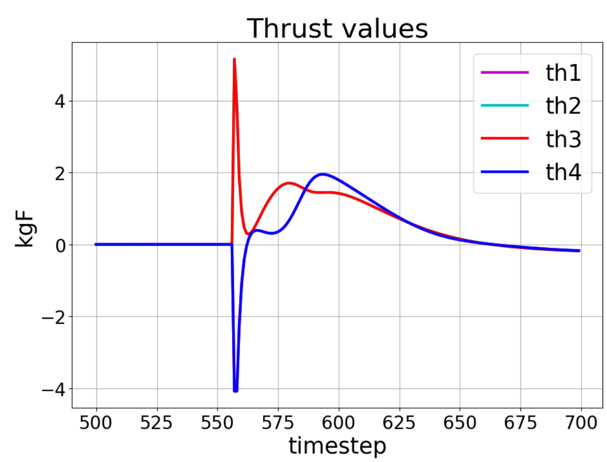

FIGURE 14: Controller effort during turning for s_c = 0.001

To analyse the effect of neglecting the controller cost, s_c was set to 0 in (9a) and the corresponding plot of controller effort for the same set of waypoints is shown in Figure 15 along with a magnified view of controller effort at turn in Figure 16. It can be noted by comparing Figure 14 and Figure 16 that, even a small factor for consideration of controller cost can significantly improve the overall efficiency.

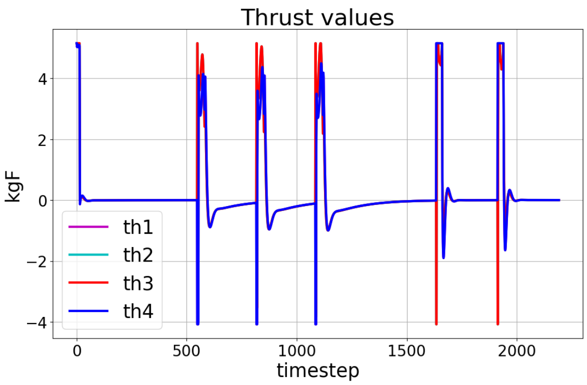

FIGURE 15: Controller effort when s_c = 0

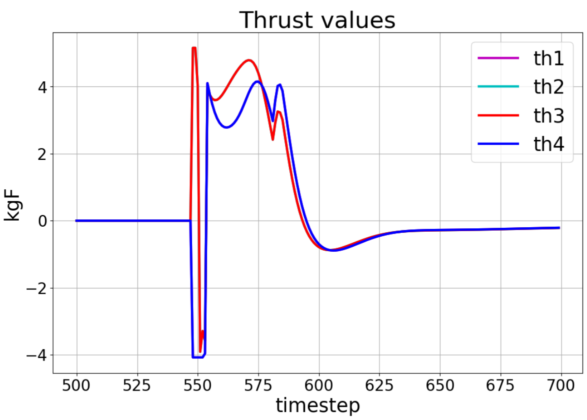

FIGURE 16: Controller effort during turning for s_c = 0

Furthermore, the effect of actuating using more commands from the sequence of optimal actions provided by MPC was also analysed. Figure 17 shows the plot of controller effort when first 2 control actions were actuated from each evaluation of MPC. A magnified view of the controller effort at turn for the same case is shown in Figure 18. It can be noted here that the control effort sequence from MPC has oscillations in values for the diagonally opposite thrusters. Since no thruster rate constraint was imposed in the formulation of MPC, the actions in the sequence generated are essentially treated as independent by the optimization process and this leads to oscillations. Such oscillations are undesirable for practical considerations so in the present study, only the first action from the sequence will be considered and its simulations will be compared against experiments.

6. CONCLUSION

This paper presents a holistic overview of system identification and a subsequent formulation of MPC. Using just free running experiments with no prior knowledge about the vessel's parameters, the maneuvering model of the vessel is identified. This identified model is used for simulating the vessel trajectory for open loop control inputs and it is compared against unseen

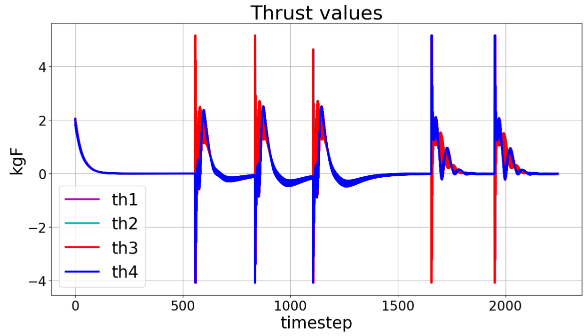

FIGURE 17: Controller effort with s_c = 0.001 and 2 control actions being chosen from each evaluation of MPC

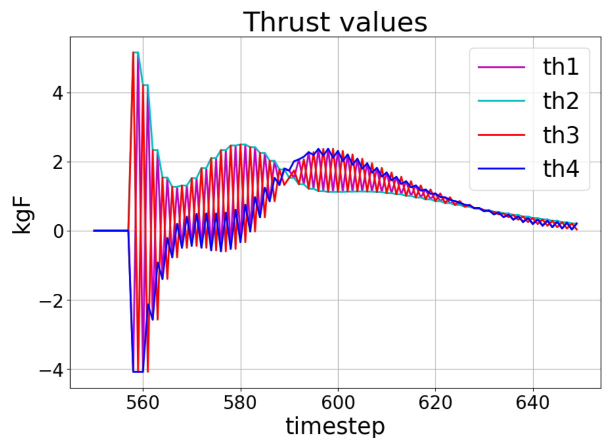

FIGURE 18: Controller effort during turning with s_c = 0.001 and 2 control actions being chosen from each evaluation of MPC

trajectory from the experiments. Along with the formulation of MPC, its potential as a method to better evaluate the accuracy of the identified model is also suggested in subsection 5.1.

In future, more free running trajectory data will be collected to improve the accuracy of the identified model, especially with the presence of local forces in sway. MPC will be tested in experiments as explained in the formulation and it will be compared against the simulated trajectory shown.

REFERENCES

[1] Xiong, Junfeng, Gu, Feng, Li, Decai, He, Yuqing and Han, Jianda. "Design, implementation and modeling of flooding disaster-oriented usv." *Recent Advances in Robotic Systems* (2016): p. 27.

[2] Naing, Lwinthein, Ghani, Ahmad Shahril Bin Mohd, Sahalan, Muhammad Irsyad, Aziz, Mazlan Bin Abdul, Abidin, Zulkifli Zainal and Rashid, Muhammad Mahbubur. "Development and fieldwork trial of autonomous surface vehicles for bathymetry mapping." *2017 IEEE 7th International Conference on Underwater System Technology: Theory and Applications (USYS)*: pp. 1–5. 2017. IEEE.

[3] Devaraju, Abhilash, Chen, Linying and Negenborn, Rudy R. "Autonomous surface vessels in ports: Applications, technologies and port infrastructures." *Computational Logis-*

tics: 9th International Conference, ICCL 2018, Vietri sul Mare, Italy, October 1–3, 2018, Proceedings 9: pp. 86–105. 2018. Springer.

[4] Souza, Luiz FM, Lopes, Gabriel SV, Uenojo, Aléxis K, Silva, Humberto T, Campopiano, Fábio, de Melo, Márcio R, Frutuoso, Adriano BS, Silva, Daniele CL, Pellini, Eduardo L and Barros, Ettore A. "Development of an asv trimaran for testing and implementation of auv navigation algorithms." *IFAC-PapersOnLine* Vol. 55 No. 31 (2022): pp. 184–189.

[5] Pandey, Jyotsna and Hasegawa, Kazuhiko. "Study on manoeuverability and control of an autonomous Wave Adaptive Modular Vessel (WAM-V) for ocean observation." *2015 International Association of Institutes of Navigation World Congress (IAIN)*: pp. 1–7. 2015. IEEE.

[6] Yoshimura, Yasuo, Masumoto, Yumiko et al. "Hydrodynamic database and manoeuvring prediction method with medium high-speed merchant ships and fishing vessels." *International MARSIM Conference*: pp. 1–9. 2012.

[7] Yasukawa, Hironori and Yoshimura, Y. "Introduction of MMG standard method for ship maneuvering predictions." *Journal of marine science and technology* Vol. 20 (2015): pp. 37–52.

[8] Araki, Motoki, Sadat-Hosseini, Hamid, Sanada, Yugo, Tanimoto, Kenji, Umeda, Naoya and Stern, Frederick. "Estimating maneuvering coefficients using system identification methods with experimental, system-based, and CFD free-running trial data." *Ocean Engineering* Vol. 51 (2012): pp. 63–84.

[9] Afram, Abdul and Janabi-Sharifi, Farrokh. "Theory and applications of HVAC control systems–A review of model predictive control (MPC)." *Building and Environment* Vol. 72 (2014): pp. 343–355.

[10] Salem, Fawzan and Mosaad, Mohamed I. "A comparison between MPC and optimal PID controllers: Case studies." (2015).

[11] Mahipala, Dhanika and Johansen, Tor Arne. "Model Predictive Control for Path Following and Collision-Avoidance of Autonomous Ships in Inland Waterways." *2023 31st Mediterranean Conference on Control and Automation (MED)*: pp. 896–903. 2023. IEEE.

[12] Omerdic, Edin and Roberts, Geoff. "Thruster fault diagnosis and accommodation for open-frame underwater vehicles." *Control engineering practice* Vol. 12 No. 12 (2004): pp. 1575–1598.

[13] Mohan, Anand and Sharma Somayajula, Abhilash. "Analyzing Robustness and Accuracy of Different Controllers for Underactuated Ships." *2023 4th International Conference for Emerging Technology (INCET)*: pp. 1–6. 2023. DOI 10.1109/INCET57972.2023.10170098.

[14] Fossen, Thor I. *Handbook of marine craft hydrodynamics and motion control*. John Wiley & Sons (2011).

[15] Abkowitz, Martin A. "Measurement of hydrodynamic characteristics from ship maneuvering trials by system identification." Technical report no. 1980.

[16] Deogaonkar, Vallabh Vinod, Jadhav, Aditya Kailas, Ramachandran, Krishnavelu and Somayajula, Abhilash Sharma. "Data Driven Identification of Ship Maneuvering Coefficients." *International Conference on Offshore Mechanics and Arctic Engineering*, Vol. 86878: p. V005T06A050. 2023. American Society of Mechanical Engineers.

[17] Ramachandran, Krishnavelu, Borsutkar, Visharad and Somayajula, Abhilash Sharma. "Comparison Between Experiments and Simulations for a Ship Maneuvering in Waves." *International Conference on Offshore Mechanics and Arctic Engineering*, Vol. 86878: p. V005T06A044. 2023. American Society of Mechanical Engineers.

[18] Li, Qiang, Li, Ranyang, Ji, Kaifan and Dai, Wei. "Kalman Filter and Its Application." *2015 8th International Conference on Intelligent Networks and Intelligent Systems (ICINIS)*: pp. 74–77. 2015. DOI 10.1109/ICINIS.2015.35.

[19] BlueRobotics. "BlueRobotics." (2024). URL https://bluerobotics.com/. Accessed on 10 January 2024.

[20] Duchon, Claude E. "Lanczos filtering in one and two dimensions." *Journal of Applied Meteorology and Climatology* Vol. 18 No. 8 (1979): pp. 1016–1022.

[21] Andersson, Joel A E, Gillis, Joris, Horn, Greg, Rawlings, James B and Diehl, Moritz. "CasADi – A software framework for nonlinear optimization and optimal control." *Mathematical Programming Computation* (2018).

[22] Jorge, Vitor AM, Granada, Roger, Maidana, Renan G, Jurak, Darlan A, Heck, Guilherme, Negreiros, Alvaro PF, Dos Santos, Davi H, Gonçalves, Luiz MG and Amory, Alexandre M. "A survey on unmanned surface vehicles for disaster robotics: Main challenges and directions." *Sensors* Vol. 19 No. 3 (2019): p. 702.